University of Birmingham

Research at Birmingham

Unfastening of hexagonal headed screws by a collaborative robot

Li, Ruiya; Pham, Duc; Huang, Jun; Tan, Yuegang; Qu, Mo; Wang, Yongjing; Kerin, Mairi; Jiang, Kaiwen; Su, Shizhong; Ji, Chunqian; Liu, Quan; Zhou, Zude

Unfastening of Hexagonal Headed Screws by a Collaborative Robot

Ruiya Li, Duc Truong Pham, Jun Huang, Yuegang Tan, Mo Qu, Yongjing Wang, Mairi Kerin, Kaiwen Jiang, Shizhong Su, Chunqian Ji, Quan Liu, and Zude Zhou

Abstract— **Disassembly is a core procedure in remanufacturing. Disassembly is currently carried out mainly by human operators. It is important to reduce the labor content of dis-assembly through automation, to make remanufacturing more economically attractive. Threaded fastener removal is one of the most difficult disassembly tasks to be fully automated. This article presents a new method developed for automating the unfastening of screws. An electric nutrunner spindle with a geared offset adapter was fitted to the end of a collaborative robot. The position of a hexagonal headed screw in a fitted stage was known only approximately, and its orientation in the hole was unknown. The robot was programed to perform a spiral search motion to engage the tool onto the screw. A control strategy combining torque and position monitoring with active compliance was implemented. An existing robot cell was modified and utilized to demonstrate the concept and to assess the feasibility of the solution using a turbocharger as a disassembly case study.**

Note to Practitioners—**Remanufacturing is known to generate substantial economic, social, and environmental benefits. Disassembly is the first operation in a remanufacturing process chain. Unfastening threaded parts ("unscrewing") is a common disassembly task accounting for approximately 40% of all disassembly activity. Like other disassembly tasks, often, unscrewing has to be carried out manually in remanufacturing due to difficulties caused by the variable and unpredictable condition of the end-of-life (EoL) products to be remanufactured. Automat-ing unscrewing operations should reduce the labor content of disassembly, thus lowering remanufacturing costs and promoting the adoption of remanufacturing. This article proposes the use of a collaborative robot to perform autonomous unfastening of hexagonal headed screws. Collaborative robots have built-in force sensors and can be programed to carry out operations involving not only position but also active force and compliance control. They can work safely alongside human operators, enabling the latter to focus on jobs requiring high cognitive or manipulation abilities. The article presents a novel spiral search technique developed to improve the rate of successful engagement between the robot end effector and the screw heads despite uncertainties in the location of the screws. The technique was successfully demonstrated on the dismantling of a turbocharger but can readily be applied to other EoL products with hexagonal headed screws. It can also be used with other kinds of screws (e.g., Phillips screws and slotted-head screws) simply by changing the tool and tuning the robot control parameters. A limitation of the proposed technique is that it can only deal reliably with undamaged screws. In our future research, we will consider screws that are in imperfect conditions through usage and develop appropriate solutions for their removal by robots.**

I. INTRODUCTION

REMANUFACTURING is a process that turns end-of-life (EoL) products into products that are equivalent to, or better than, newly manufactured products, prolonging their working life [1]. Remanufacturing operations normally include product disassembly, cleaning, inspection, repair, replacement, reassembly, and testing. Remanufacturing supports environmental and economic sustainable development goals [2]. However, insufficient automation has been identified as potentially limiting the growth of this sector [3].

Disassembly is an early process step in the remanufacturing value stream. The variability in shape, dimensions, and condition of EoL products poses challenges for the disassembly automation [4]. Consequently, disassembly tends to be done manually, utilizing the flexibility of humans. However, this has a lower efficiency than automated methods and is associated with higher labor costs [5].

Existing research in remanufacturing automation focuses on reducing manual operations through the realization of optimal robotic and autonomous disassembly [6]–[10]. Optimizing disassembly sequences and investigating disassembly fundamentals are two current areas of research. In disassembly sequence planning (DSP), finding the optimal sequence is key to reducing processing time and cost [11]–[15]. Once optimized, the disassembly plan can be executed. Disassembly operations may include removing shafts from clearance fit bores, unfastening threaded fasteners, extracting interference-fit components, removing elastic parts (o-rings, circlips, etc.),

R. Li is with the Department of Mechanical Engineering, School of Mechanical and Electronic Engineering, Wuhan University of Technol-ogy, Wuhan 430070, China, and also with the Department of Mechanical Engineering, School of Engineering, University of Birmingham, Birmingham B15 2TT, U.K. (e-mail: liruiya@whut.edu.cn).

D. T. Pham, J. Huang, M. Qu, Y. Wang, M. Kerin, K. Jiang, S. Su, and C. Ji are with the Department of Mechanical Engineering, School of Engineering, University of Birmingham, Birmingham B15 2TT, U.K. (e-mail: D.T.Pham@bham.ac.uk; J.Huang.1@bham.ac.uk; mxq360@student.bham.ac.uk; Y.Wang@bham.ac.uk; MEK790@student.bham.ac.uk; KXJ797@student.bham.ac.uk; S.Su.2@bham.ac.uk; C.Ji@bham.ac.uk).

Y. Tan and Z. Zhou are with the Department of Mechanical Engineering, School of Mechanical and Electronic Engineering, Wuhan University of Technology, Wuhan 430070, China (e-mail: ygtan@whut.edu.cn; zudezhou@whut.edu.cn).

Q. Liu is with the Department of Automation, School of Information Engineering, Wuhan University of Technology, Wuhan University of Tech-nology, Wuhan 430070, China (e-mail: quanliu@whut.edu.cn).

and separating permanently mated subassemblies (those that are nailed, glued, welded, riveted, stapled, soldered together, etc.). Investigating disassembly operations from a fundamental perspective can provide useful information that can guide process design. However, so far there has been little work on this, although for common operations, such as removing a shaft from a bore it may be possible to use some of the results of previous studies on the reverse process of inserting the shaft into the bore [16]–[18].

Threaded fasteners (screws, bolts, and hybrids) are widely employed to form mechanical connections in consumer goods and mechanical equipment. They are generally used to hold two or more parts together in a semipermanent stage permit-ting disassembly by removing the fastener. The unfastening of screws and the unscrewing of bolts are key disassembly activities where automation can be applied. Jia *et al.* [19] review the state of the art in threaded fastener automation for assembly processes and discuss fastening strategies. It is not possible to use or adapt fastening strategies directly for unfastening, as the processes of fastening in assembly and unfastening for disassembly are not the same, nor are they simply the reverse of each other.

In fully automated fastening assembly stations, new threaded screws/bolts are often fed into the equipment with mechanisms designed to orientate and locate them ready for fitment. The fitting tool (screwdriver, wrench, nutrunner, spin-dle with socket, etc.) runs down the fastener, having knowledge of its position and perhaps orientation. If the orientation is unknown, flexibility in the tool manages the initial engage-ment, before programing ensures uniform torque strategies are applied (often using a snug state before triggering the final tightening process). Engagement of the socket on the fastener happens when the fastener has some freedom in its movement. The transducer on the rotating tool initially experiences low torque. As the threads of the fastener engage on those in the mating part, and as stretch occurs, the transducer can measure an increase in torque and/or angle and evaluate the results against a predefined criterion.

In unfastening, the orientation and position of the fastener are less certain due to the initial assembly process variation and the effects of in-life utilization. Engagement between the socket and the fastener can occur when the fastener is free to move (not properly fitted), or more probable at EoL, when the fastener has very little opportunity to move (fully fitted). This makes the positioning of the tool more critical than in the fastening scenario. The torque requirements are at their highest at the start of the unfastening process and reduce as the fastener returns to nominal length, and the threads disengage. The torque experienced at the end of the unfastening process is low, and identifying when the threads have completely disengaged is more complex. This drives the requirement to devise a new control strategy specific to automated unfastening.

Data on the location of a product's fasteners can be extracted from computer-aided design (CAD) software or identified using a vision system [20]–[23]. However, there are sev-eral errors in both methods that affect the alignment of the CAD/vision system data with reality. These include the following:

1) machining tolerance buildup in the real product that is not reflected in the CAD model;
2) acceptance of nonconformances in real products not identified in the CAD model;
3) real product in-use size/shape changes due to exposure to forces/temperatures, etc., not reflected in the CAD model;
4) real product in-use modifications not reflected in the CAD model;
5) dirt, rust or corrosion buildup not reflected in the CAD model;
6) calculations and filtering applied to vision systems not reflecting reality.

The above can impact the fixturing of the EoL product, which in turn affects its positioning in the disassembly cell. Combined with the remanufacturing equipment errors (back-lash, robot motion, flexing, under loading, etc.), positioning and alignment errors between the socket and the fastener are highly likely.

In 1998, Apley *et al.* [24] used a dc electrical tool and data acquisition system to obtain unfastening torque and angle plots for different screws before categorizing them into four states:

1) screw coming out (OK = 0);
2) screwdriver slipping on the head of a screw (NOK = 1);
3) screwdriver missed screw (NOK = 1);
4) screw too tight to move (NOK = 1).

From these states, a condition detection algorithm was developed and demonstrated to support automated decision making. However, the solution to the NOK states was not reported. In 2001, Seliger *et al.* [25] presented a disassembly tool with a pneumatic end effector to grasp the top surface of the screw head. Later in 2002, Zuo *et al.* [26] reported a "screw nail" end effector that can drill into the screw head to realize self-connection. Both of Seliger *et al.*'s tools first grasp the screw head by generating new acting surfaces on the screw head, and then start to rotate to unfasten the screw. These methods do not require the tools to be well aligned with the screws before unscrewing. However, the connection between the tools and screws is not as strong as for traditional tools (screwdriver, wrench, nutrunner, spindle with socket, etc.). If the screws to be removed were tightly fastened in the product, these two tools may fail to work. In 2014 and 2015, Chen *et al.* [27], [28] built an unscrewing robot to assist humans in electric vehicle batteries disassembly. The focus of their work was the tool changing procedure, and they did not provide the details of the unscrewing process. In 2018, Mironov *et al.* [29] developed a methodology for robotic unscrewing using data extracted from skilled human opera-tors. They studied force conditions in manual screwing and unscrewing operations, and proposed a force-based control strategy. They did not report on how to locate the screws and how to judge the success of their removal. Also, in 2018, DiFilippo and Jouaneh [30] presented a robotic system that combined force and vision sensing to assist with the removal of Philips head screws from laptops. A computer vision mod-ule was used to locate screw holes, and an accelerometer was mounted on the screwdriver to determine the completion of the unfastening process. DiFilippo and Jouaneh's work focused on

Fig. 1. Disassembly process for one screw.

establishing and testing the computer vision module, aiming to find the screws in the products automatically without preprograming their locations. The effects of varying light levels and the brightness of the products on the performance of the vision module in the proposed system were analyzed. For the screws that were found by the vision module, the sensor-equipped screwdriver removed them with a success rate of 96.5% (251/260). The position error between the tool and the screws was not considered. How the engagement of the tool with the screw head and the completion of the unfastening were assessed was not discussed in detail.

In this article, we first analyze the entire unscrewing process and divide it into four stages in Section II. A spiral search strategy is presented that was designed to compensate for initial socket-screw positioning errors and to ensure engagement. A control strategy that combines position control, force control, and active compliance mode, is proposed for automated screw unfastening. In Section III, the robotic unscrewing system developed is described together with the test con-ducted to validate the proposed method. Finally, a case study in human–robot collaborative disassembly demonstrating the proposed automated unscrewing method/solution is presented in Section IV.

II. METHODS AND STRATEGIES FOR AUTOMATED UNFASTENING OF THREADED SCREWS

A. Method for Automated Removal of One Screw

The automated removal of one threaded screw is composed of four stages, including approach, search and engage, unfasten, and assess and leave (shown in Fig. 1). The details and

corresponding control method of each stage are presented in the following.

1) Approach: The approximate position and the centerline of the screw in a component are extracted from an applicable CAD model or using a vision system. The robot equipped with the unfastening tool moves to a position above the screw. The tool rotates slowly in the fastening direction, and the robot is programed to switch into active compliance mode. The rotation of the tool is initially in the fastening direction to ensure that any loose screw will be tightened up a given torque before the actual unfastening stage begins. The tool is moved toward the screw along the estimated centerline until contact is made with the screw head. If the tool and screw are perfectly aligned, engagement will be achieved automatically without the need to carry out the next stage.

2) Search and Engage: In the more likely scenario where the tool and screw are not aligned, a search and engage step needs to be initiated. A spiral motion is adopted that involves moving outward from the estimated center of the screw, as shown in Fig. 1. The tool continues to rotate slowly in the fastening direction while orbiting. Once the tool and screw engage, there is a sudden increase in robot joint torques seen by the robot controller and in the torque measured by the tool transducer.

3) Unfasten: The robot equipped with the tool continues to operate in the active compliance mode. Once the target tighten-ing torque has been reached, indicating successful engagement between the tool and the screw, the robot stops the spiral search motion. The tool then starts to rotate in the unfastening
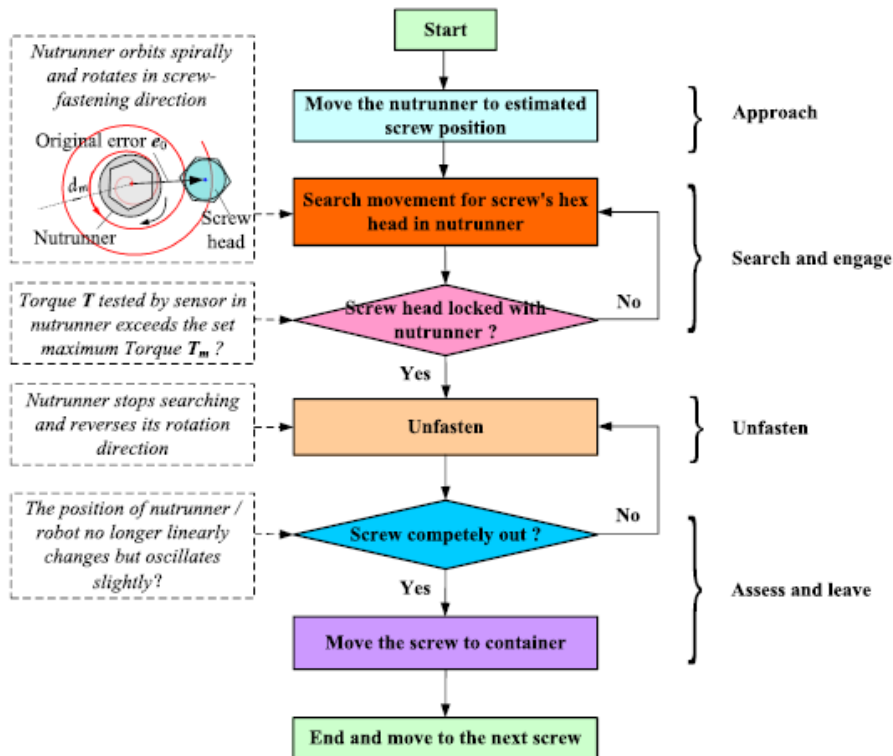

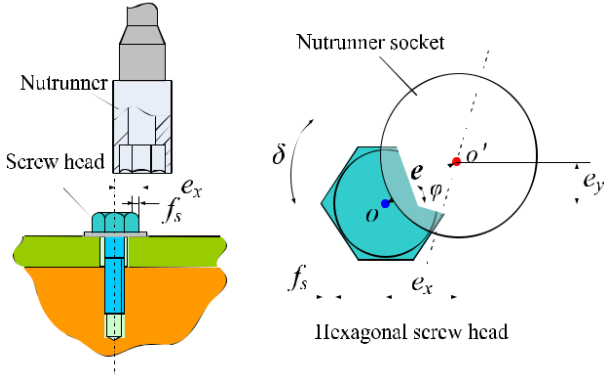Fig. 1. Disassembly process for one screw.

Fig. 2. Positional error between the screw and tool.

Fig. 3. Engagement condition.

direction, and the robot moves away from the hole following the screw during run-out.

4) Assess and Leave: While unfastening, the torque measured by the tool transducer falls, then toward the end, it fluctuates. This makes it difficult to be certain that the screw threads are free from those in the hole using force feedback. It is then proposed to use the robot's positioning information. Due to the geometry of threaded screws, there is a relationship between rotation, thread pitch, and distance fitted/extracted in a full $360°$ rotation. The robot maintains a constant force in the axial direction on the tool, which, in turn, maintains a constant force in the axis direction on the screw. The robot arm follows the feed movement of the screw being unfastened from the product. Once all the threads on the screw have been separated from those in the threaded hole in the product, the feed movement of the screw stops, although it still keeps rotating. Meanwhile, due to the chamfer at the end of the screw threads, as it rotates, the screw oscillates slightly along its axis. Therefore, if it is detected that the robot arm no longer moves linearly in the screw's axis direction but displays oscillating movements when the screw keeps rotating, the screw is presumed to be free from the threaded hole. The process is now complete.

B. Spiral Search Strategy for Threaded Hexagonal Headed Screw

When the tool mounted on the robot moves to the expected position of the fitted screw, there exists a positional error $e = \overrightarrow{O\,O}$, as shown in Fig. 2. The magnitude and direction of $\overrightarrow{O\,O}$ are unknown. The maximum magnitude e_{max} of $\overrightarrow{O\,O}$ can be influenced by the accuracy of the robot motion or the machine vision system (if used). The direction of $\overrightarrow{O\,O}$ can be any angle ϕ between $0°$ and $360°$. Due to the uncertainty of $\overrightarrow{O\,O}$, a spiral search method has been developed to ensure the screw head is always located. More precisely, the distance between the centerline of the tool end effector and the screw should be small enough to ensure complete coverage and eventual alignment. Meanwhile, there exists an angular error δ ($0° \le \delta \le 60°$) between the tool, and the screw head orientation (in this article it is the error between the hexagonal hole in the geared offset adapter and the hexagonal head of the screw).
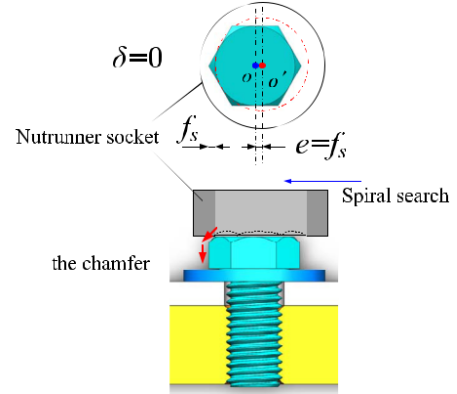
It is, therefore, necessary for the tool to continue to rotate during the spiral orbit. For calculating the equation of the spiral orbit, the fitting condition between the tool and the screw head should first be defined.

It can be seen from Fig. 2 that the screw head is chamfered, forming a circle on the top surface. f_S represents the chamfer size that increases relative to the screw's size. Additionally, the hexagon edges scribe a larger parallel circle when rotated. The area between these two circles is defined as the chamfer area with center O. Similarly, the tool head edges scribe a circle with center O when rotated. Under the conditions that $O = O$ and $\delta = 0$, the fastening tool would locate onto the screw head without any necessary correction. If $O = O$ but $\delta = 0$, the circles are aligned, the tool will not locate and will instead sit on top of the screw head. Rotation of the tool with respect to the screw head is required for engagement to occur.

In fact, when the magnitude of the error is small enough ($e \le f_S$, not necessarily $e = 0$), the nutrunner can slide down through the chamfer and fit with the screw head under the precondition $\delta = 0$, as shown in Fig. 3. Therefore, the objective function, namely, the engagement condition can be expressed as

$$e = \overline{\underset{\delta}{=}0.}\, \sqrt{e_x^2 + e_y^2} \le f_S \qquad (1)$$

Constraints now need to be defined. The distance d_m between different circles of the spiral orbit should first be considered. A small d_m prolongs the search time, while a large d_m would result in missing the fitting condition. The maximum distance d_m should be $d_m = 2 f_S$, to minimize search time, as shown in Fig. 4. The velocity v_{orbit} of the tool should also be determined. Like d_m, a small v_{orbit} also prolongs the search time, while an excessive v_{orbit} would result in missing the fitting condition. When the tool moves with a velocity v_{orbit} at a distance $2 f_S$ in a spiral orbit, it should also rotate at an angle larger than $60°$ (assuming a hexagon head and socket arrangement) to ensure $\delta = 0$ and $e \le f_S$ could be realized simultaneously when the tool is close enough to the screw head to engage, as shown in Fig. 5. If the rotating speed of the tool is n_S (rev/min), it takes $10/n_S$ (s) to rotate 1/6 of a
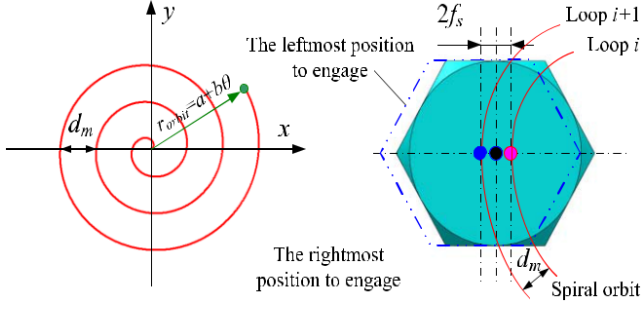
Fig. 4. Maximum distance d_m between different circles of the spiral orbit.
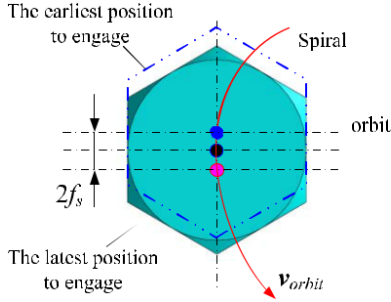
Fig. 5. Maximum velocity v_{orbit} of the spiral movement.

turn ($60°$). v_{orbit} should be

$$v_{orbit} \leq \frac{2 f_s}{10/n_s} = \frac{n_s f_s}{5}. \qquad (2)$$

In polar coordinates, the spiral orbit can be expressed as $r_{orbit} = a + b\theta$, as shown in Fig. 4, where a and b are constant. Therefore, the distance d_m between different loops of the spiral orbit is

$$d_m = r_{orbit}|_{\theta=2(k+1)\pi} - r_{orbit}|_{\theta=2k\pi}$$
$$= 2\pi \cdot b, \quad k = 1, 2, 3, \dots. \qquad (3)$$

According to the previous discussion, we can determine that $b = d_m/2\pi = f_s/\pi$. Since the value of a has no effect on the shape of the spiral path, we can assume that $a = 0$. As θ increases with time t, so that the orbiting velocity v_{orbit} remains constant, it can be shown that

$$\theta(t) = \beta\sqrt{t}. \qquad (4)$$

Consequently, the spiral orbit can be expressed as

$$r_{orbit} = \frac{f_s}{\pi}\beta\sqrt{t}. \qquad (5)$$

In Cartesian coordinates, it can be expressed as

$$x = \frac{f_s}{\pi}\beta\sqrt{t}\cos(\beta\sqrt{t})$$
$$y = \frac{f_s}{\pi}\beta\sqrt{t}\sin(\beta\sqrt{t}). \qquad (6)$$

The orbiting velocity can be expressed as

$$v_{orbit} = \frac{ds_{orbit}}{dt} = \frac{r_{orbit}d\theta}{dt} = \frac{\frac{f_s}{\pi}\beta\sqrt{t}d\beta\sqrt{t}}{dt} = \frac{f_s\beta^2}{2\pi}. \qquad (7)$$

Comparing (7) with (2), we can obtain

$$\beta = \sqrt{\frac{2\pi n_s}{5}}. \qquad (8)$$

Therefore, the determined spiral orbit is

$$x = \frac{f_s}{\pi}\sqrt{\frac{2\pi n}{5}t}\cos\left(\sqrt{\frac{2\pi n}{5}}t\right)$$
$$y = \frac{f_s}{\pi}\sqrt{\frac{2\pi n}{5}t}\sin\left(\sqrt{\frac{2\pi n}{5}}t\right).$$

Assuming the magnitude of the initial error is e_0, the numbers of the orbit laps N_{orbit} needs to be

$$N_{orbit} \geq \frac{e_0}{d_m}, \quad N_{orbit} \in \mathbf{N}. \qquad (10)$$

$\mathbf{N}$ represents the natural number set. Correspondingly, the time required to complete N_{orbit} laps should be

$$\sqrt{\frac{2\pi n_s}{5}t} = 2\pi \cdot N_{orbit}. \qquad (11)$$

Therefore, the maximum spiral search time t_{max} can be expressed as

$$t_{max} = \frac{10\pi}{n_s} \cdot \text{ceil}\left(\frac{e_0}{2 f_s}\right)^2 \qquad (12)$$

where ceil is the ceiling math function. If $n_s = 60$ rev/min, and the initial position error between the screw head and the nutrunner socket is $e_0 = 2.5$ mm, the maximum search time for hexagonal headed screws of different sizes is shown in Table I.

It can be seen from Table I that, with the same initial error, the larger the screw, the lower the search time. If the initial error e_0 is less than 1 mm and the rotating speed n_s of the nutrunner is 60 rev/min, the maximum search times for M4, M6, and M10 screws are all 0.52 s according to (12). It can be seen from Fig. 6, that the spiral searching method is sufficient to cover the area needed to ensure engagement between the tool and the screw. Higher orbiting velocity and shorter search times can be achieved when the rotating speed of the tool increases. However, there is a greater probability of failure, and a balance between confidence levels and speed needs to be found.
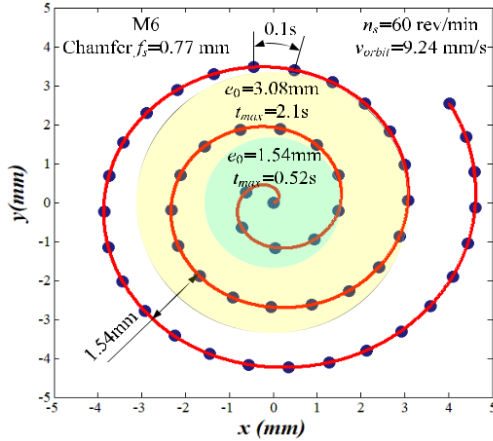
Fig. 6.   Search time of M6 screw with different initial errors.

C. Active Compliance

Many uncontrollable factors exist in the unfastening of threaded screws, as already described. Additional factors include the original tightening stage, the use of lubricants, sealants or compounds during fitment, and screw/product damage. During the unfastening process, there are strong inter-action forces between the tool and the screw. If the movement of the tool is rigid, it may fail to complete the operation and could cause damage to the product, tool, or robot. The system needs to be flexible enough to allow for the search motion to occur with contact expected between the screw head and the tool surface, then to follow the movement of the screw out of the product.

As shown in Fig. 7(a), the tool needs to move toward the screw along its axis from the original position (O_1) to the target position O_2. Therefore, the robot is controlled to move downward a distance d_z. However, due to positional errors in the perpendicular plane, the tool will touch the screw head in position O_3, generating a virtual compression λ in the robot arm, which results in contact force between the tool and the screw head. As the tool starts its search orbit, static and dynamic friction forces are experienced. In order to deal with these different forces, there is a requirement to maintain a level of elasticity in the robot-tool system.

Once the tool aligns with the screw, it needs to start the spiral search to engage the screw head fully. In the same way, as shown in Fig. 7(b), when the screw is being removed, the head will move away from the product. Elasticity in the robot-tool system will support these process steps. When the screw moves up a distance h, the robot arm will be correspondingly pushed to move up a distance $d = h$. This elasticity can be achieved in two ways. First, an elastic-mechanical connection between the tool and the robot can be integrated. Alternatively, the robot's active compliance mode can be utilized by setting stiffness and damping factors that influence the robot's joint behavior. The latter approach was adopted in this article.

III. Experimental Results and Discussion

An experimental cell was designed and realized, to validate the developed method and strategy for automated unfastening.
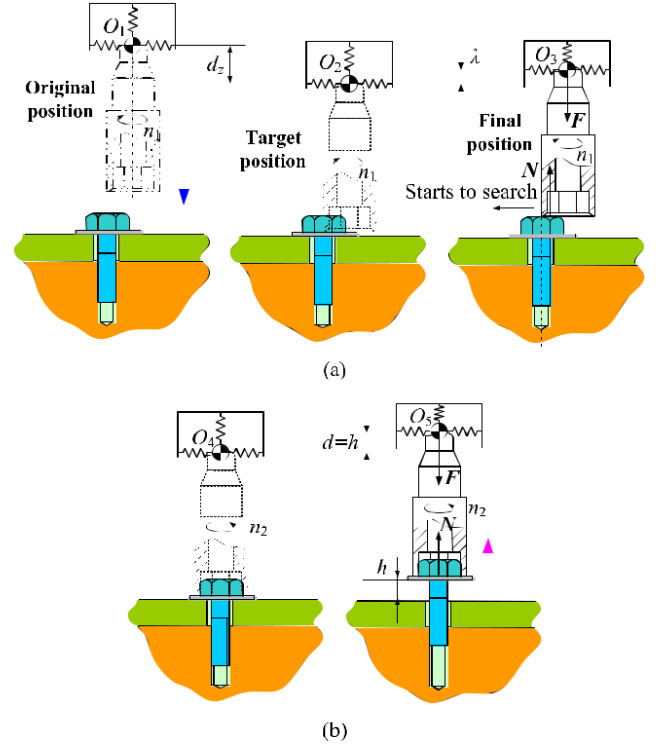
Fig. 7. Elasticity needed in the robotic screw unfastening system. (a) Touching on the screw head top face and searching. (b) Following the unfastening movement.
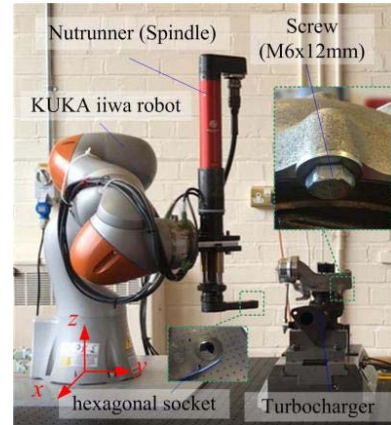
Fig. 8.   Experimental setup.

The product to be disassembled was an automotive tur-bocharger. The fastener was a hexagonal headed screw with integrated washer. The robot-tool system used to unfasten the screw was a modified electrical nutrunner fixed to an industrial collaborative robot with an active compliance control function. Experiments were completed as per the setup, procedures, and parameters documented in Section III-A and III-B, respec-tively, with results presented in Section III-C.

A. Experimental Setup

Fig. 8 shows the experimental setup and equipment. An electrical nutrunner (Georges Renault SASMC51-10) fitted with a geared offset M6 (Lubbering) adapter was installed on the end flange of an industrial collaborative robot (KUKA LBR

iiwa 14 R800). The nutrunner controller was programed to set the rotating speed, direction, and torque load settings. The socket in the adapter was designed to handle an M6 hexagonal headed screw. The collaborative robot was controlled by the KUKA Sunrise system.

Compared to traditional industrial robots, collaborative robots have force sensing capabilities to ensure the safety of humans. They can work in active compliance control mode with configurable stiffness and damping. The robot program was written in Java in the KUKA Sunrise Workbench platform.

Real-time sensing information collected by the robot, including force, torque, and position, was used to support the unfastening process. The nutrunner controller was connected to the KUKA Sunrise Cabinet, enabling the stop/start operation of the spindle to be integrated. A hexagon headed screw (M6 × 12 mm) fitted to the compressor housing of an EoL automotive turbocharger (BorgWarner 54359710029) was used. A pneumatic vice (Schunk, TANDEM KSP-LH PLUS 250) was employed to secure the turbocharger.

B. Procedure for Automated Unfastening

The flowchart of the control procedure is shown in Fig. 9. Initially, the robot moved the tool, aligning the adapter center hole with the estimated center of the screw 1 mm from the head face. Once in position, the tool began to rotate at low speed (n_1) in the tightening direction controlled by phase **D** in Table II. "Intertime" is the time between two consecutive phases. The robot's active compliance mode was switched on, and the robot moved toward the product until the tool touched the screw head. Then, the robot started the spiral search path

		Max time	90 s
Inter-time	0 s	Inter-time	0 s
Target torque	10 Nm	Min torque	1 Nm
Rotating direction	CCW	Target torque	15 Nm
Speed	25 rev/min	Max torque	20 Nm
		Rotating direction	CW
		Speed	100 rev/min

until the tool engaged with the screw head. For different unscrewing stages, the robot's 6-DOF stiffnesses were set to different values, as shown in Table III.

1) Assess the Engagement of the Tool With the Screw Head Using Force Control: The upper fastening torque limit of the nutrunner was set at 10 Nm at a rotating speed n_1. Once the fastening torque exceeded the upper limit, which meant the tool had engaged with the screw head, the tool reversed (rotated in the unfastening direction) with speed n_2 controlled by phase **F** in Table II, as illustrated in Fig. 10. Simulta-neously, the force and torque experienced by the tool were transferred to the robot arm. Force-based control of the robot is a reliable way to determine tool-screw head engagement. Fig. 11 shows the 6-DOF dynamic forces/torques at the base of the robot during the unfastening process. Fig. 11(a) and (c), respectively, displays the 3-DOF forces and 3-DOF torques for
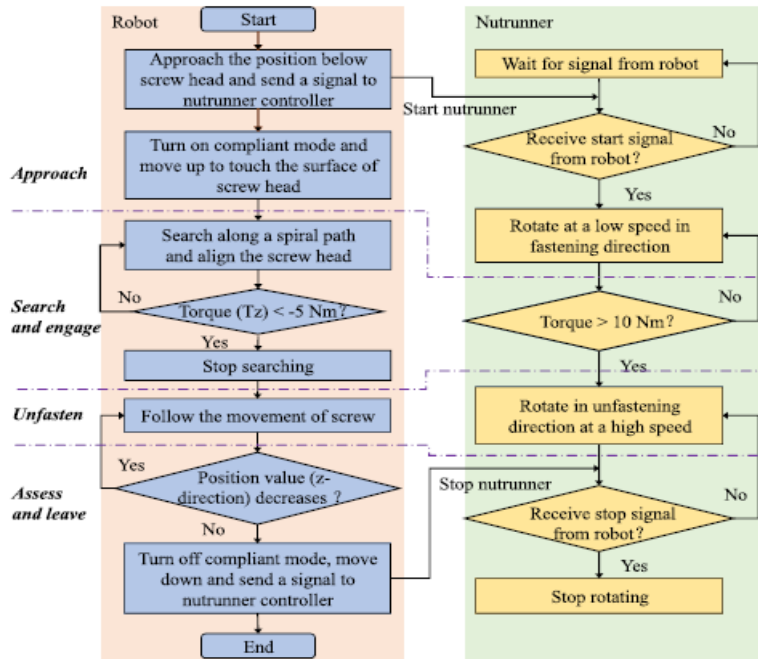

Fig. 9. Flowchart of control procedure [31].

TABLE III
STIFFNESS SETTING FOR ROBOT ARM

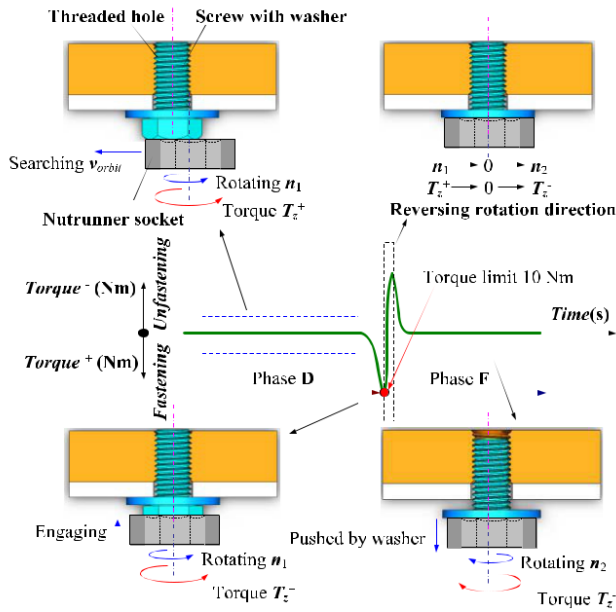|		Approach before touching	Search & engage	Unfasten & assess	Leave
Translational stiffness (N/m)	X	2000	3500	50	2000
	Y	2000	3500	50	2000
	Z	2000	2000	10	2000
Rotational stiffness (Nm/rad)	X	200	100	10	200
	Y	200	100	10	200
	Z	200	100	10	200

Fig. 10.   Torque in the process of searching → engaging → unfastening.

the entire process, while Fig. 11(b) and (d) shows enlarged views of Fig. 11(a) and (c) for the first two seconds. From Fig. 11(b) and (d), it can be seen that force in the x-direction and torque in the z-direction were highest when the tool engaged with the screw head at the end of stage 2, as the engagement of tool with screw head obstructed the spiral movement of the tool in the x-direction and the rotation of the tool around the z-direction. Here, the torque in the z-direction was chosen to be utilized in the force-based control system to assess the engagement of the tool with the screw head. Due to friction losses, the torque limit programed into the robot in the z-axis was set to −5 Nm. Exceeding this limit triggered the end of the spiral search motion of the robot arm and the start of unfastening. Alternatively, the torque signal from the nutrunner's controller could be used, but in this experiment, it was not used as there was no output port to pass the information to the robot controller. Using the torque signal measured by the robot to control the motion was the most effective and economical solution available for this work.

2) Assess the End of Unfastening Using Position Control: It can also be seen from Fig. 11(a) and (c) that, for stage 3, the torque in the nutrunner experienced a downward trend. At the end of this stage, the torque fluctuated at a very

low level. It was difficult to judge whether the screw was completely out of the threaded hole according to the magnitude change of the force/torque. Although the characteristics of the force/torque changed a little after the screw was completely unfastened, and through feature extraction and comparison of the force/torque signals, the end of the unfastening operation could be determined, the procedure would be too complex and time-consuming. Compared with the force/torque signal, the robot position along the z-axis exhibited much more easily distinguishable trends before and after the screw was out of the threaded hole. Fig. 12 illustrates the position change of the screw and robot-tool system in the z-direction in the unfastening process. As shown in Fig. 12(a), the rotation of the screw driven by the nutrunner results in friction between threads on the screw and those in the threaded hole. The resultant force F_{thread} of the tangential frictional force and the normal force on the threaded surface of the threaded hole, push the screw and the robot-tool system downward, away from the product. After all the threaded part of the screw is out of the threaded hole, the screw stops moving downward although it still keeps rotating. As shown in Fig. 12(b), because of the support force F_{support} from the robot, the top of the screw keeps contact with the mouth of the threaded hole. As the thread at the top of the screw and that on the chamfer of the threaded hole are incomplete, the screw moves up and down along the z-axis periodically when it rotates. Fig. 13 shows the test results. The traversing of the screw during unfastening forces the robot-tool system to move downward away from the product. Although the slope of the position drop (in the z-direction) along time is not constant due to the tiny tilt between the nutrunner axis and threaded hole axis, the robot-tool system keeps moving downward without a sudden rise during unfastening. After the screw is free from the threaded hole, the screw periodically oscillates when it rotates. There-fore, the jump of the tool in the z-direction can be used to judge the end of the unfastening stage. Once the positioning profile indicates that the robot position in the z-direction no longer linearly decreases but there is a jump in the position, it could be assumed that the screw is then free from the threaded hole in the product. A stop signal is sent to the nutrunner by the robot controller to stop the rotation, the active compliance mode is switched off, and the robot is then used to move the screw to the container.

C. Results and Discussion

The methodology, control procedures, and parameters implemented in the experimental system are shown in Fig. 8. The estimated center of the screw was taught to the robot by the human operator. In order to verify the spiral search method, the computer intentionally created random position errors for the robot before it started to touch the screw and unfasten it. The screw was unfastened and removed 98 times successfully in 100 consecutive trials, with a random initial position error e ($0 \leq e \leq 3$ mm, $0° \leq \phi \leq 360°$) between the tool and the screw generated by the computer in each trial. Fig. 14 presents images taken of the entire process of a successful trial. Fig. 14(a) shows the start position of the nutrunner with respect to the turbocharger before it moved to
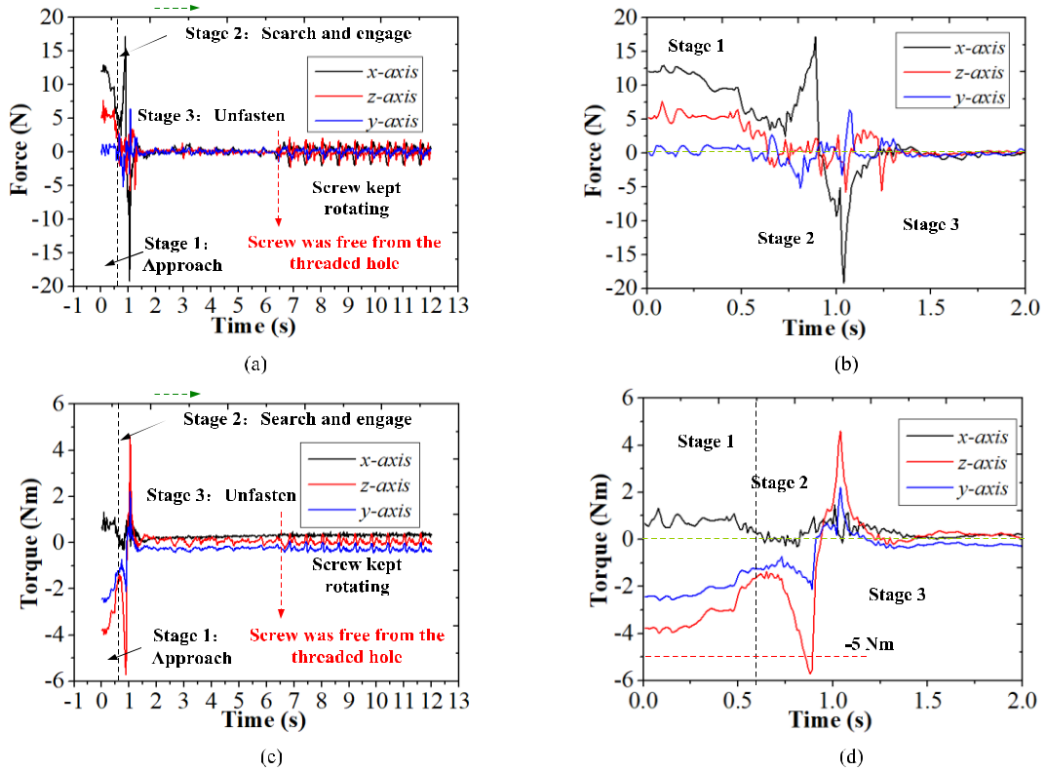
Fig. 11. 6-DOF force measured at the base of the robot. 3-DOF forces for (a) entire process and (b) first 2 s. 3-DOF torques for (c) entire process and (d) first 2 s.
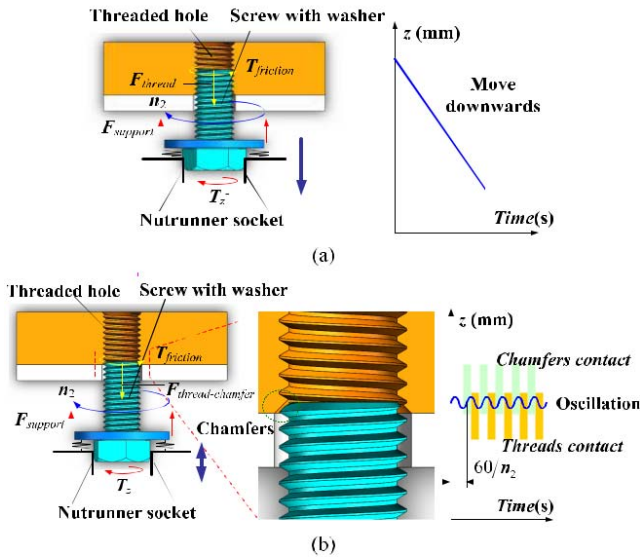
Fig. 12. Position (in the *z*-axis) of the screw and robot-tool system in unfastening. (a) Moving downward during unfastening. (b) Oscillating when the screw is free from the threaded hole.

1 mm below the screw head [Fig. 14(b)]. Fig. 14(c) shows the tool touching the surface of the bolt head and the spiral search path in progress, and then the tool is pictured engaging with the screw in Fig. 14(d). The unfastening of the screw and the movement of the tool away from the turbocharger housing can be seen in Fig. 14(e). Complete disengagement is shown in Fig. 14(f) and in (g). Finally, the screw was taken away by the robot [Fig. 14(h)].

Fig. 13. Position feedback in the robot. Position change in *z*-direction (a) for the entire process and (b) from 5.5 to 9.0 s.

As shown in Fig. 15, during the "approach" stage, the tool moved upward from its original position. It then stopped at contact with the screw head (point A). The "search and

Fig. 14. Automated unfastening of a screw in a turbocharger: (a) initial position, (b) approach, (c) search, (d) engage, (e) unfasten, (f) assess, (g) leave, and (h) transport.

Fig. 15.   Torque and position feedback measured by the robot.

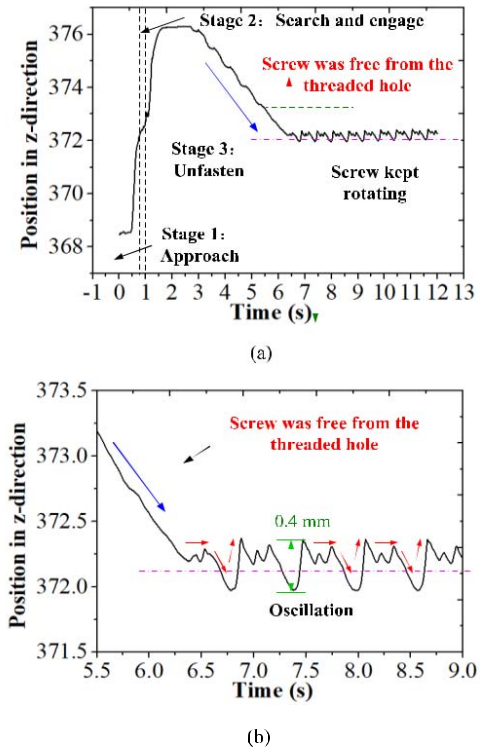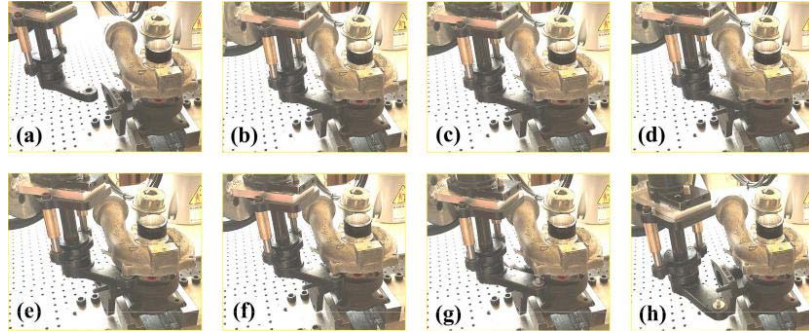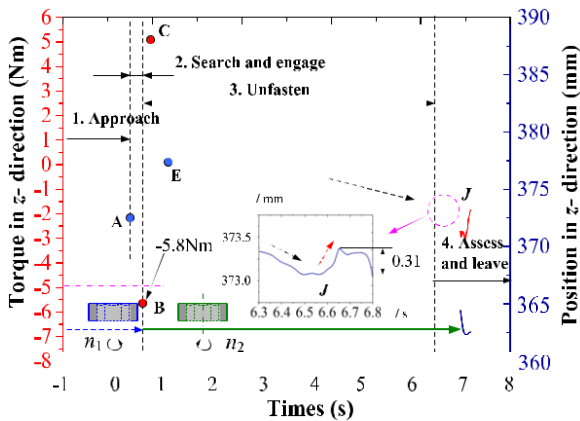engage" stage lasted around 0.32 s during which time the tool rotated in the fastening direction, moving along the spiral path, retaining contact with the screw head. The position of the tool remained relatively stable in the z-direction. Engagement between the tool and the screw started shortly before point B, where the torque in the z-direction fell suddenly to -5.8 Nm exceeding the -5-Nm limit. This triggered the stopping of the spiral search and the start of the rotation in the unfastening direction. Before the rotation was reversed, torque peaked at point C as engagement had started, and tightening was still being applied. The tool continued to move toward the product, and engagement was not complete until point E. Displacement in the z-axis gradually fell after point E as the screw run-out forced the tool away from the turbocharger housing. Oscillation of the torque from point E correlated with the number of threads on the screw (nine). The untightening process was assumed complete when the 0.31-mm jump of the tool in the z-direction was detected. It was this displacement and position assessment that was used to trigger the end of the unfastening process, assuming the screw was now free from the hole. The oscillations from 6.8 to 7.2 s were caused by movement in the robot, not from the unfastening feedback.

IV. APPLICATION TO HUMAN–ROBOT COLLABORATIVE DISASSEMBLY OF AN AUTOMOTIVE TURBOCHARGER

A. Structure of the Automotive Turbocharger

The turbocharger assembly was made up of impellers (compressor and turbine), a shaft, bearings, and bushes, a housing,
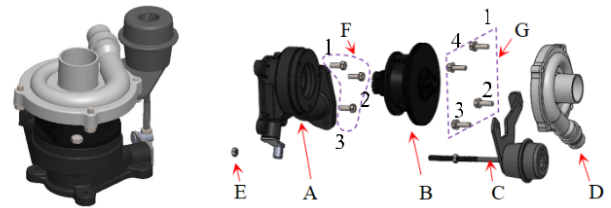

Fig. 16.   Turbocharger and components.

and a wastegate actuator. These parts were held together using fasteners (primarily screws) accessible from the outside. Turbochargers experience high temperature differentials dur-ing their lifetime. In extreme conditions they can fall below -40 °C when not in use, and above 700 °C during normal operation depending on the application and environmental con-ditions. Combined with the high working pressures, rotating speeds, and various exhaust gas particulates, the internals of the turbocharger (impellers, shaft, bearings, etc.) reach the EoL before the housing and actuator. The option to reuse the housing and actuator with new internals makes remanufac-turing of turbochargers desirable. Cost-efficient separation of these components is key to maximizing profits. The process of disassembly is detailed using an example (Fig. 16). The main components and fasteners are listed in Table IV.

B. Disassembly Sequence Planning

According to the assembly relationships between the four main components (A–D) and following observation of the manual disassembly process in the remanufacturing facility, a DSP was derived (Fig. 17). As A–D need to be separated, the whole disassembly process can be divided into three stages. In the first stage, the actuator (C) is removed by unfastening screws G1, G2, and G3, and nut E. In the second stage, screws G4 are unfastened before the turbine housing is separated from the impeller (B). Finally, screws F1, F2, and F3 are removed to separate the impeller (B) from the turbine housing (A).

C. Human–Robot Collaborative Disassembly of the Turbocharger

The robotic manufacturing provides superior consistency and efficiency over human operators performing similar

TABLE IV
MAIN COMPONENTS AND FASTENERS OF THE TURBOCHARGER

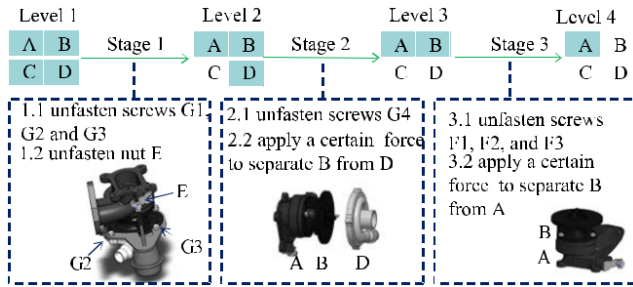|						
	Impeller with pedestal	Steel and others	×	F	Screw	M6x15
C	Wastegate actuator	Steel	√	G	Screw	M6x12
D	Compressor housing	Aluminum alloy	√			

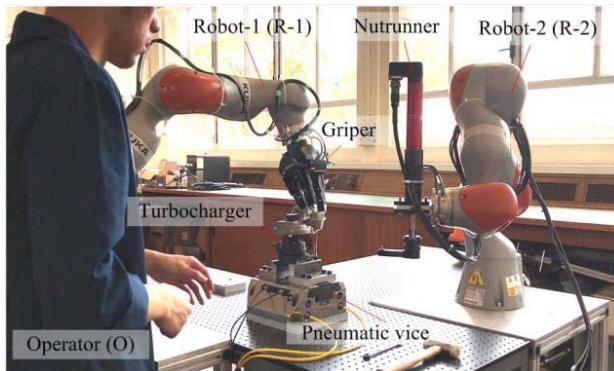Fig. 17. Disassembly sequence plan for the turbocharger.

Fig. 18. Human–robot collaborative disassembly system.

repetitive tasks. They can also be used in hazardous environ-ments or where there is a risk to human health/safety. However, some tasks remain too complex for robots or too expensive to automate. Humans are still preferred when high-level strategic decision making, or dexterity, is required. Combining the benefits of both the human and robot in a human–robot collab-orative system is seen as the manufacturing future [32]–[35].

The robot can carry out, considering the disassembly of the turbocharger, many of the required operations. However, some are better suited to humans depending on the situation, complexity, and time. To complete the disassembly of the turbocharger, a human–robot collaborative disassembly cell was designed.

As shown in Fig. 18, the cell consisted of two robots (KUKA LBR iiwa 14 R820) and a human operator. The end effector of Robot-1 was a three-finger adaptive gripper (ROBOTIQ) employed to handle the components and fas-teners. Robot-2's end effector was the electrical nutrunner and adapter mentioned in Section III-B and used to unfasten

accessible screws. The operator interacted with the robot and performed some disassembly tasks that the robot could not handle because of difficulties with access. A pneumatic vice was used to secure the turbocharger, and a fixture was employed to help the three-finger gripper handle the cast turbocharger housing. Once disassembled, the individual com-ponents are transferred to separate containers.

According to the analysis in Section IV-B, to separate the four main components, seven screws (G1, G2, G3, G4, F1, F2, and F3) and one nut (E) had to be unfastened. Screws G1, G2, G3, and G4 could be accessed and removed using the developed automated unfastened solution. However, screws F1, F2, and F3 were inaccessible to the robot due to their positioning with respect to interfering surfaces. Additionally, the position of nut E along the actuator shaft was variable, and the subassembly was unstable, making it more suited to human disassembly. Therefore, screws F1, F2, and F3 and nut E were processed manually.

The detailed disassembly operations are shown in Fig. 19, with each step allocated to the human operator (O), the two collaborative robots (R-1, R-2), or a combination. Robot-1 (handling) was involved in 12/17 operations, Robot-2 (unfas-tening) in 6/17, and the human operator in 4/17. The tur-bocharger was successfully disassembled in 3 min and 13 s. The entire disassembly process can be viewed by following the link in the Appendix.

Robot-1 used a fixture to hold onto the turbocharger hous-ing, moving it to between the jaws of the pneumatic vice. The vice closed around the turbocharger securing its position. Robot-2 then unfastened screw G1. Once the screw had been completely freed, Robot-2 moved away from the turbocharger, and Robot-1 picked the screw from Robot-2 and dropped it in the relevant container. This process was repeated for screw G2. The unfastening of screw G3 by Robot-2 was subtly different, as Robot-1 was required to hold onto the actuator to improve stability. Once screw G3 had been removed, Robot-1 continued to hold the actuator so that the human operator could unthread nut E. With all fasteners connecting the actuator to the turbocharger housing removed, the operator pressed down on the robot to give it the command to continue with the disassembly process. Robot-1 took the actuator to the relevant container while Robot-2 started the unfastening of screw G4, and the process used for screw G1 and G2 was repeated.

With screws G1–G4 removed, the compressor housing was now ready to be disassembled. However, it was tightly fitted to the turbocharger housing still held by the vice, and so it

Fig. 19.   Flowchart of the turbocharger disassembly operations.

required the operator to knock it with a mallet to break it free. As Robot-1 retained its grip on the compressor housing throughout this process, the separation caused by the oper-ator lifting the housing forced the robot position to change. During this time, Robot-1 remained in active compliance mode, waiting for a signal from the operator or controller to continue the programed process. Once the change in position of Robot-1 reached a specific set of parameters, the process continued without the assistance of the operator. Robot-1 moved the compressor housing to the relevant container while the operator removed screws F1, F2, and F3 manually. Finally, Robot-1 took the impeller (part B), then the turbine housing (part A), to the relevant containers.

V. CONCLUSION

Threaded fastener removal is a difficult disassembly oper-ation fully to automate using a robotic solution. This article presents a new methodology to realize automated unfastening using a collaborative robot equipped with an adapted electrical nutrunner. A spiral search strategy is discussed that was developed to align, locate, and engage a nutrunner onto a hexagon headed fastener with an initial positional error. Tests were conducted on one fastener to validate and demonstrate the feasibility of the proposed process. This provided torque and displacement data that supported the development of an unfastening control strategy combining torque control, position control, and active compliance. Finally, a collaborative cell and process designed to disassemble a turbocharger, utilizing the proposed automated unfastening solution, was described.

The developed method has three issues requiring attention: 1) when the tool touches the screw head, and the robot searches for the position to engage, friction between the screw head surface and the tool affects the kinematic accuracy of the spiral movement, which could lead to the failure of the engagement between the tool and the screw head; 2) the torque limit set in the robot for assessing the engagement between the tool and

the screw head is lower than that in the nutrunner controller due to transmission losses from the tool to the robot arm. The torque limit in the robot needs to be set according to actual situations; 3) the developed strategy can only be used to unfasten screws in good conditions; possible failures of the screw (screw stuck, screw head damaged, etc.) were not considered.

Future work will focus on addressing the above issues by optimizing the search strategy and integrating machine vision to improve the success rate of engagement between tool and screw head at stage 2. The torque signal in the nutrunner controller will be extracted to replace the torque signal in the robot to assess the engagement. More experiments will be carried out, and possible failure modes of the designed method will be investigated to enhance its robustness.

APPENDIX

1) As θ increases with t, we can assume

$$\theta(t) = \beta\, t^{\eta}. \tag{13}$$

From (5) and (7)

$$v_{\text{orbit}} = \frac{ds_{\text{orbit}}}{dt} = \frac{r_{\text{orbit}}d\theta}{dt} = \frac{\frac{f_s}{\pi}\beta\, t^{\eta}\, d\beta\, t^{\eta}}{dt} = \frac{f_s\beta^2 t^{2\eta-1}}{\pi}. \tag{14}$$

The orbiting velocity v_{orbit} is constant only when $\eta = 1/2$.

2) The turbocharger disassembly described in Section IV can be viewed in a video on YouTube at: https://www.youtube.com/watch?v=kOwGe_LbLzs.

REFERENCES

[1] S. Bernard, "Remanufacturing," *J. Environ. Econ. Manage.*, vol. 62, no. 3, pp. 337–351, Nov. 2011.

[2] V. D. R. Guide, Jr., "Production planning and control for remanufacturing: Industry practice and research needs," *J. Oper. Manage.*, vol. 18, no. 4, pp. 467–483, Jun. 2000.

[3] J. Kurilova-Palisaitiene, E. Sundin, and B. Poksinska, "Remanufacturing challenges and possible lean improvements," *J. Clean. Prod.*, vol. 172, pp. 3225–3236, Jan. 2018.

[4] R. Gerbers, K. Wegener, F. Dietrich, and K. Dröder, "Safe, flexible and productive human-robot-collaboration for disassembly of lithium-ion batteries," in *Recycling Lithium-Ion Batteries*. Cham, Switzerland: Springer, 2018, pp. 99–126.

[5] S. Vongbunyong, S. Kara, and M. Pagnucco, "A framework for using cognitive robotics in disassembly automation," in *Proc. 19th CIRP Conf. Life Cycle Eng., Leveraging Technol. Sustainable World*, Berkeley, CA, USA, May 2012, pp. 173–178.

[6] S. Vongbunyong, S. Kara, and M. Pagnucco, "Application of cognitive robotics in disassembly of products," *CIRP Ann.-Manuf. Techn.*, vol. 62, no. 1, pp. 31–34, 2013.

[7] S. Vongbunyong, S. Kara, and M. Pagnucco, "Learning and revision in cognitive robotics disassembly automation," *Robot. Comput.-Integr. Manuf.*, vol. 34, pp. 79–94, Aug. 2014.

[8] E. Minca, A. Filipescu, and A. Voda, "Modelling and control of an assembly/disassembly mechatronics line served by mobile robot with manipulator," *Control Eng. Pract.*, vol. 31, pp. 50–62, Oct. 2014.

[9] S. Vongbunyong and W. H. Chen, "Disassembly automation," in *Sustainable Production, Life Cycle Engineering Management*. Cham, Switzerland: Springer, 2015, pp. 25–54.

[10] J. Li, M. Barwood, and S. Rahimifard, "Robotic disassembly for increased recovery of strategically important materials from electrical vehicles," *Robot. Comput.-Integr. Manuf.*, vol. 50, pp. 203–212, Apr. 2018.

[11] Y. Xing, C. Wang, and Q. Liu, "Disassembly sequence planning based on Pareto ant colony algorithm," *J. Mech. Eng.*, vol. 48, no. 9, pp. 186–192, Sep. 2012.

[12] H.-P. Hsu, "A fuzzy knowledge-based disassembly process planning system based on fuzzy attributed and timed predicate/transition net," *IEEE Trans. Syst., Man, Cybern. Syst.*, vol. 47, no. 8, pp. 1800–1813, Aug. 2017.

[13] Y. Luo, Q. Peng, and P. Gu, "Integrated multi-layer representation and ant colony search for product selective disassembly planning," *Comput. Ind.*, vol. 75, pp. 13–26, Jan. 2016.

[14] J. Liu *et al.*, "An improved multi-objective discrete bees algorithm for robotic disassembly line balancing problem in remanufacturing," *Int. J. Adv. Manuf. Tech.*, vol. 97, nos. 9–12, pp. 3937–3962, Jun. 2018.

[15] Y. Feng *et al.*, "Target disassembly sequencing and scheme evaluation for CNC machine tools using improved multiobjective ant colony algorithm and fuzzy integral," *IEEE Trans. Syst., Man, Cybern. Syst.*, to be published.

[16] M. W. Abdullah *et al.*, "An approach for peg-in-hole assembling using intuitive search algorithm based on human behavior and carried by sensors guided industrial robot," *IFAC-PapersOnline*, vol. 48, no. 3, pp. 1476–1481, 2015.

[17] H. C. Song, Y. L. Kim, and J. B. Song, "Automated guidance of peg-in-hole assembly tasks for complex-shaped parts," in *Proc. IEEE/RSJ Int. Conf. Intell. Robot. Syst.*, Chicago, IL, USA, Sep. 2014, pp. 4517–4522.

[18] I. F. Jasim, P. W. Plapper, and H. Voos, "Position identification in force-guided robotic peg-in-hole assembly tasks," *Procedia CIRP*, vol. 23, no. 23, pp. 217–222, 2013.

[19] Z. Jia, A. Bhatia, R. M. Aronson, D. Bourne, and M. T. Mason, "A survey of automated threaded fastening," *IEEE Trans. Autom. Sci. Eng.*, vol. 16, no. 1, pp. 298–310, Jan. 2019.

[20] U. Büker *et al.*, "Vision-based control of an autonomous disassembly station," *Robot. Auton. Syst.*, vol. 35, nos. 3–4, pp. 179–189, Jun. 2001.

[21] P. Gil, J. Pomares, S. T. P. C. Diaz, F. Candelas, and F. Torres, "Flexible multi-sensorial system for automatic disassembly using cooperative robots," *Int. J. Comput. Integ. Manuf.*, vol. 20, no. 8, pp. 757–772, Jun. 2008.

[22] S. R. Cruz-Ramirez, Y. Mae, T. Takubo, and T. Arai, "Detection of screws on metal-ceiling structures for dismantling tasks in buildings," in *Proc. IEEE/RSJ Int. Conf. Intell. Robot. Syst.*, Nice, France, Sep. 2008, pp. 4123–4129.

[23] M. Bdiwi, A. Rashid, and M. Putz, "Autonomous disassembly of electric vehicle motors based on robot cognition," in *Proc. IEEE Int. Conf. Robot. Automat. (ICRA)*, Stockholm, Sweden, May 2016, pp. 2500–2505.

[24] D. W. Apley, G. Seliger, L. Voit, and J. Shi, "Diagnostics in disassembly unscrewing operations," *Int. J. Flex. Manuf. Syst.*, vol. 10, no. 2, pp. 111–128, 1998.

[25] G. Seliger, T. Keil, U. Rebafka, and A. Stenzel, "Flexible disassembly tools," in *Proc. IEEE Int. Symp. Electron. Environ.*, Denver, CO, USA, May 2001, pp. 30–35.

[26] B. R. Zuo, A. Stenzel, and G. Seliger, "A novel disassembly tool with screwnail endeffectors," *J. Intell. Manuf.*, vol. 13, no. 3, pp. 157–163, 2002.

[27] W. H. Chen, K. Wegener, and F. Dietrich, "A robot assistant for unscrewing in hybrid human-robot disassembly," in *Proc. IEEE Int. Conf. Robot. Biomimetics (ROBIO)*, Bali, Indonesia, Dec. 2014, pp. 536–541.

[28] K. Wegener, W. H. Chen, F. Dietrich, K. Dröder, and S. Kara, "Robot assisted disassembly for the recycling of electric vehicle batteries," *Procedia CIRP*, vol. 29, pp. 716–721, Apr. 2015.

[29] D. Mironov, M. Altamirano, H. Zabihifar, A. Liviniuk, V. Liviniuk, and D. Tsetserukou, "Haptics of screwing and unscrewing for its application in smart factories for disassembly," in *Haptics: Science, Technology, Applications*. Cham, Switzerland: Springer, 2018, pp. 428–439.

[30] N. M. Difilippo and M. K. Jouaneh, "A system combining force and vision sensing for automated screw removal on laptops," *IEEE Trans. Autom. Sci. Eng.*, vol. 15, no. 2, pp. 887–895, Apr. 2018.

[31] J. Huang *et al.*, "A screw unfastening method for robotic disassembly," in *Proc. Int. Conf. Sustain. Smart Manuf. (S2M)*, Manchester, U.K., Apr. 2019, pp. 1–6.

[32] V. Villani, F. Pini, F. Leali, and C. Secchi, "Survey on human-robot collaboration in industrial settings: Safety, intuitive interfaces and applications," *Mechatronics*, vol. 55, pp. 248–266, Nov. 2018.

[33] X. V. Wang, Z. Kemény, J. Váncza, and L. Wang, "Human-robot collaborative assembly in cyber-physical production: Classification framework and implementation," *CIRP Ann.*, vol. 66, no. 1, pp. 5–8, 2017.

[34] Q. Liu, Z. Liu, W. Xu, Q. Tang, Z. Zhou, and D. T. Pham, "Human-robot collaboration in disassembly for sustainable manufacturing," *Int. J. Prod. Res.*, vol. 57, no. 12, pp. 1–18, Feb. 2019.

[35] H. Cheng, W. Xu, Q. Ai, Q. Liu, Z. Zhou, and D. T. Pham, "Manufacturing capability assessment for human-robot collaborative disassembly based on multi-data fusion," *Procedia Manuf.*, vol. 10, pp. 26–36, Jun. 2017.

Ruiya Li received the B.E. degree in mechanical engineering from the Wuhan University of Technology, Wuhan, China, in 2012, where he is currently pursuing the doctoral degree with the Optical Fiber Sensing Group.

He is currently researching with the Autonomous Remanufacturing Laboratory, University of Birmingham, Birmingham, U.K., as a Joint Ph.D. Candidate. His main research interests include fiber Bragg grating sensing technology, and robotic disassembly.

Duc Truong Pham holds the Chance Chair of Engineering at the University of Birmingham where he started his career as a lecturer in robotics and control engineering following undergraduate and postgraduate studies at the University of Canterbury in New Zealand. Prior to returning to Birmingham in 2011, he was Professor of Computer-Controlled Manufacture and Director of the Manufacturing Engineering Centre at Cardiff University. His research is in the areas of intelligent systems, robotics and autonomous systems and advanced manufacturing technology.

Jun Huang received the B.E., M.E., and Ph.D. degrees in mechanical engineering from the Wuhan University of Technology, Wuhan, China, in 2010, 2013, and 2017, respectively.

He is working as a Research Fellow with the School of Engineering, University of Birmingham, Birmingham, U.K. His research interests include optical fiber sensor, autonomous remanufacturing, cutting force measurement, robotics, and condition monitoring.

Yuegang Tan received the B.E. and M.E. degrees from Chongqing University, Chongqing, China, in 1983 and 1989, respectively, and the Ph.D. degree from the Wuhan University of Technology, Wuhan, China, in 2005.

He is currently a Professor with the School of Mechanical and Electronic Engineering, Wuhan University of Technology. His research interests include robot and its control, control theory and applications, and machinery equipment dynamic monitoring technology and application.

Mo Qu received the M.E. degree in mechanical engineering from the University of Birmingham, Birmingham, U.K., in 2017, where he is currently pursuing the Ph.D. degree with the School of Engineering.

His current research interests include manufacturing, robotics and automation, reinforcement learning and optimization.

Yongjing Wang received the B.Eng. degree (Hons.) in electrical and electronic engineering from the University of Birmingham, Birmingham, U.K., in 2013, the B.Eng. degree in automation from the Harbin Institute of Technology, Harbin, China, in 2013, and the Ph.D. degree in engineering from the University of Birmingham, in 2016.

He is currently a Research Fellow with the Autonomous Remanufacturing Laboratory (ARL), University of Birmingham. His active research is in automation systems with an emphasis on robotic disassembly. He has been leading the design and developments of several robotic disassembly systems at Birmingham.

Dr. Wang is a fellow of the Higher Education Academy, a member of the Institute of Technology, and a Winner of a Royal Society International Exchange Award in 2019.

Mairi Kerin received the M.Eng. DIS degree (Hons.) from Loughborough University, Loughborough, U.K. She is currently pursuing the Ph.D. degree in mechanical engineering in the area of digital systems for remanufacturing with the University of Birmingham, Birmingham, U.K.

She worked as a Manufacturing Projects Engineer with Caterpillar, Inc., Peoria, IL, USA, and Jaguar LandRover, Coventry, U.K., over a 10-year period, primarily focused on the design, installation, and commissioning of green field engine test facilities in the U.K. and in India. Her research is funded by the EPSRC and the Manufacturing Technology Centre (MTC).

Kaiwen Jiang received the B.S. degree in mechanical design, manufacture and automation from the North China University of Technology, Beijing, China, in 2017, and the M.S. degree in advanced mechanical engineering from the University of Birmingham, Birmingham, Birmingham, U.K., in 2018, where she is currently pursuing the Ph.D. degree in mechanical engineering.

Her research interests include the CAD model information extraction, human–robot work distribution, disassembly sequence replanning, and robotic bolt unscrewing process generator and optimizing.

Shizhong Su has been with the School of Mechanical Engineering, Jilin University, Changchun, China, since 1985. As a Project Manager and a Researcher, he has been involved in a number of EU/EPSRC projects on advanced manufacturing and remanufacturing technology. He is currently a Senior Research Fellow with the Department of Engineering, University of Birmingham, Birmingham, U.K. He has authored more than 50 articles in journals and international conferences on high-tech advanced manufacturing and computer-aided engineering.

Chunqian Ji received the Ph.D. degree in system engineering from the University of Wales, Cardiff, U.K., in 2004.

He is currently a Senior Research Fellow with the University of Birmingham, Birmingham, U.K. His research interests include intelligent systems, CAD/CAM, 3-D printing, rapid tooling, sensors and control, automation of machines, manufacturing information systems, laser micromachining, composite materials, self-healing materials, autonomous disassembly, remanufacturing, robotics, and circular economy.

Quan Liu received the B.Eng. degree from the Department of Electronic and Information, Huazhong University of Science and Technology, Wuhan, China, in 1985, and the M.Eng. and Ph.D. degrees from the Department of Automation, Wuhan University of Technology, Wuhan, in 1991 and 2004, respectively.

She is currently a Chief Professor with the School of Information Engineering, Wuhan University of Technology. Her research interests include signal processing, signal detection, and digital manufacturing.

Zude Zhou received the B.Eng. degree in electric power system and automation from the Huazhong University of Science and Technology, Wuhan, China, in 1970, and the Doctor of Engineering degree from the University of Birmingham, Birmingham, U.K., in 2015.

He is currently a Chief Professor of Mechanical Engineering with the School of Mechanical and Electronic Engineering, Wuhan University of Technology, Wuhan. He has authored over 300 articles in academic journals and conferences and more than ten monographs. His research interests include digital manufacturing, advanced manufacturing technology, digital monitoring and fault diagnosis.

Dr. Zhou is a Foreign Member of the Russian Academy of Engineering and a fellow of the Society of Manufacturing Engineers.